

Weak disorder in photonic crystals

© M. Artoni^{1,2}, S.A.R. Horsley³, G.C. La Rocca⁴

¹ Department of Engineering and Information Technology, Brescia University, Brescia, Italy

² European Laboratory for Nonlinear Spectroscopy, Sesto Fiorentino, Italy

³ School of Physics and Astronomy, University of Exeter, Exeter, United Kingdom

⁴ NEST, Scuola Normale Superiore, Pisa, Italy

e-mail: giuseppe.larocca@sns.it

Received June 12, 2024

Revised June 12, 2024

Accepted July 29, 2024

Finite one-dimensional photonic crystals with geometric and compositional disorder are studied via a perturbative approach in the weak effective disorder limit. Our model gives expressions that, when used to compute disorder-averaged reflectivity spectra around the photonic band gap, yield accurate results and significantly more efficiently than through a direct numerical average over disorder realization. The method is specially suited to deal with atomic photonic crystals with low levels of disorder and a substantial number of periods.

Dedication: We are honored to dedicate this paper to the memory of Professor Vladimir Agranovich. We have always been deeply inspired by his paramount scientific achievements and his enthusiasm for physics. One of us (G.C.L.R.) is deeply and forever indebted to Professor Agranovich for his constant encouragement, help and friendship over many years.

Keywords: photonic crystal, disorder, distributed Bragg reflector, photonic stop band.

DOI: 10.61011/EOS.2024.08.60027.6782-24

1. Introduction

Photonic crystals of various kinds provide a useful toolbox in optics and spectroscopy for tailoring light-matter interactions [1]. These systems are characterized by a periodic spatial modulation of their dielectric response on a length scale comparable to the wavelength of light, leading to the opening of stop bands (energy gaps) in the photonic density of states. The simplest example is a periodic stack of quarter-wavelength plates, realizing a distributed Bragg reflector [2].

This sort of one-dimensional photonic crystal can be realized not only using solid state components, but also using cold atoms loaded into an optical lattice, where the atomic density is modulated [3–5]. These latter systems have recently been much studied. Typically, a well developed photonic band gap can be realized with a rather small number of periods in a condensed matter Bragg reflector, at least when there is a high dielectric contrast between the layers. However, many more periods are required in an atomic Bragg reflector, due to the very small dielectric contrast between the atom rich and atom poor layers. Of course, the optical response of atoms can be enhanced working with a light frequency close to an atomic transition in which case, however, polaritonic effects [6] come into play and there is a non trivial interplay between the polaritonic stop band and Bragg reflection [7]; this regime

is outside the scope of the present work as only transparent media characterized by a real and frequency independent refraction index will be considered.

Another difference between condensed matter and atomic based photonic crystals is in the degree of disorder they exhibit: this is typically larger in the former [8] than in the latter [9,10]. Also, the problem of disorder induced light localization has attracted much interest [11–15], and in a multilayer system requires a scaling analysis for increasingly longer samples. In many instances, however, disorder is comparatively weak in relation to the limited size of the samples used, leading to a mild degradation of the reflectivity rather than to the appearance of localized states within the stop bands. This regime may be realized both in significantly disordered, but rather short solid state multilayers, as well as in less disordered, but much longer atomic systems, and it is clearly relevant for all practical applications of distributed Bragg reflectors.

The usual approach to deal with a finite size disordered system is a numerical simulation of the relevant physical quantities to be averaged over a large number of disorder realizations, which may be computationally demanding even for one-dimensional systems [16,17]. Here, we directly focus on the reflectivity spectra close to a photonic band gap and work out a simple shortcut to configurational averaging based on a perturbative approach to weak uncorrelated

disorder which is shown to be accurate for both geometric (i.e., positional) as well as compositional disorder [18].

2. A perturbative expansion

We begin by demonstrating that a perturbative expansion of elements of the system transfer matrix can be used to compute the disorder-averaged transmission and reflection coefficients, without having to do any time consuming numerical averaging. Consider a 1D photonic crystal of period a having a unit cell comprising a layer of thickness d with a real refractive index n and a vacuum spacer of thickness $(a - d)$. The unit cell transfer matrix M connects the forward (E_j^+) and backward (E_j^-) propagating fields in the j^{th} lattice period to those in the $(j + 1)^{\text{th}}$ period [7], and is given by

$$\begin{pmatrix} E_{j+1}^+ \\ E_{j+1}^- \end{pmatrix} = M \begin{pmatrix} E_j^+ \\ E_j^- \end{pmatrix} = \begin{pmatrix} m_{11} & m_{12} \\ m_{21} & m_{22} \end{pmatrix} \begin{pmatrix} E_j^+ \\ E_j^- \end{pmatrix} \\ = \begin{pmatrix} e^{ik_0(a-d)} & 0 \\ 0 & e^{-ik_0(a-d)} \end{pmatrix} \mathcal{M} \begin{pmatrix} E_j^+ \\ E_j^- \end{pmatrix} \quad (1)$$

with $k_0 = \omega/c$ the wave-vector in vacuum, and the transfer matrix \mathcal{M} is that for a single homogeneous layer of thickness d and refractive index n , given by

$$\mathcal{M} = \frac{1}{4n} \begin{pmatrix} (n+1)^2 e^{ik_0 d n} & (n^2-1)(e^{ik_0 d n} - e^{-ik_0 d n}) \\ -(n-1)^2 e^{-ik_0 d n} & (n+1)^2 e^{-ik_0 d n} \\ (n^2-1)(e^{-ik_0 d n} - e^{ik_0 d n}) & -(n-1)^2 e^{ik_0 d n} \end{pmatrix}. \quad (2)$$

In the ideal (no-disorder) case, the total transfer matrix of a photonic crystal containing N unit cells will be simply given by $M_T = M^N$, i.e., the product of N identical (single-cell) transfer matrices M . In the disordered case instead the single-cell transfer matrix will depend on the lattice site j and the corresponding total transfer matrix will be given by $M_T = \prod_{j=1}^N M_j$.

In the following, weak and uncorrelated disorder will be introduced, either in the refractive index (compositional disorder) or in the vacuum spacer thickness (geometric disorder). Let us consider the j^{th} cell transfer matrix M_j as a function of a real disorder parameter $p_j = p_0 + \epsilon_j$, with $\langle \epsilon_j \rangle = 0$ and $\langle \epsilon_j \epsilon_l \rangle = \delta_{jl} \epsilon^2$, where $\langle \rangle$ indicates the average over disorder realizations and $\epsilon^2 \ll p_0^2$. Then, expanding $M_j = M(p_j)$ up to second order in ϵ_j , one has the total transfer matrix,

$$M_T = \prod_{j=1}^N M_j \simeq \prod_{j=1}^N \left(M_0 + \epsilon_j M_1 + \frac{1}{2} \epsilon_j^2 M_2 \right) \quad , \quad (3)$$

where we have defined the matrices

$$M_0 = M(p_0), \quad M_1 = \left. \frac{\partial M}{\partial p} \right|_{p_0}, \quad M_2 = \left. \frac{\partial^2 M}{\partial p^2} \right|_{p_0}. \quad (4)$$

These three matrices are independent of disorder. Expanding the N -terms product (3) up to order ϵ_j^2 , we have the approximate expression

$$M_T \simeq M_0^N + \sum_{j=1}^N \epsilon_j M_0^{N-j} M_1 M_0^{j-1} + \frac{1}{2} \sum_{j=1}^N \epsilon_j^2 M_0^{N-j} M_2 M_0^{j-1} \\ + \sum_{j=1}^{N-1} \sum_{l=j+1}^N \epsilon_j \epsilon_l M_0^{N-l} M_1 M_0^{l-j-1} M_1 M_0^{j-1}. \quad (5)$$

From this total transfer matrix (5), quantities of experimental interest such as the reflectivity $R = |M_{T,12}/M_{T,22}|^2$ and transmittivity $T = |1/M_{T,22}|^2$ can be calculated [5,7] and, subsequently, averaged over many disorder realizations [10]. In the numerical examples considered below, we will assume $T + R = 1$ (no-loss).

To compute transmission, e.g., we require the matrix element $M_{T,22}$ of the total matrix in Eq. (5) which can be written in the following form

$$M_{T,22} \simeq (M_0^N)_{22} \left(1 + \sum_{j=1}^N c_j \epsilon_j + \sum_{j=1}^N \sum_{l=j}^N g_{jl} \epsilon_j \epsilon_l \right). \quad (6)$$

The numerical coefficients c_j and g_{ij} equal the ϵ_j independent combinations of matrix elements appearing within the summations in Eq. (5) and thereby do not depend on disorder. They are given by

$$c_j = (M_0^{N-j} M_1 M_0^{j-1})_{22} / (M_0^N)_{22}, \\ g_{jl} = g_{lj} = \left[\frac{1}{2} \delta_{jl} (M_0^{N-j} M_2 M_0^{j-1})_{22} \right. \\ \left. + (1 - \delta_{jl}) (M_0^{N-l} M_1 M_0^{l-j-1} M_1 M_0^{j-1})_{22} \right] / (M_0^N)_{22}. \quad (7)$$

The disorder-averaged transmission coefficient can then be written to leading order as,

$$\langle T \rangle = \left\langle \frac{1}{|M_{T,22}|^2} \right\rangle \\ \simeq \frac{1}{|(M_0^N)_{22}|^2} \left\langle \frac{1}{|1 + \sum_j c_j \epsilon_j + \sum_{j,l} g_{jl} \epsilon_j \epsilon_l|^2} \right\rangle \\ \simeq \frac{1}{|(M_0^N)_{22}|^2} \left\langle 1 - \sum_j (c_j + c_j^*) \epsilon_j \right. \\ \left. + \sum_{j,l} (c_j c_l + c_j^* c_l^* + c_j^* c_l) \epsilon_j \epsilon_l - \sum_{j,l} (g_{jl} + g_{jl}^*) \epsilon_j \epsilon_l \right\rangle \\ = T_N \left[1 + 2\epsilon^2 \text{Re} \sum_j \left(\frac{1}{2} |c_j|^2 + c_j^2 - g_{jj} \right) \right] \quad , \quad (8)$$

where $T_N = 1/|(M_0^N)_{22}|^2$ is the transmittivity of the N -layer stack in the absence of disorder ($\epsilon_j = 0$). Most importantly,

in the final step upon averaging over disorder we assume uncorrelated disorder, i.e. $\langle \epsilon_j \epsilon_l \rangle = \delta_{jl} \epsilon^2$, hence the $j \neq l$ terms can be neglected. The final expression tells us how to compute the average transmissivity in terms only of combinations of transfer matrices and their derivatives, defined in Eq. (4).

To compute reflection we require instead the ratio of two matrix elements, i.e. $M_{T,12}/M_{T,22}$. In much the same way as done for $M_{T,22}$ above, we have

$$M_{T,12} \simeq (M_0^N)_{12} \left[1 + \sum_{j=1}^N f_j \epsilon_j + \sum_{j=1}^N \sum_{l=j}^N h_{jl} \epsilon_j \epsilon_l \right], \quad (9)$$

where

$$\begin{aligned} f_j &= \frac{1}{(M_0^N)_{12}} (M_0^{N-j} M_1 M_0^{j-1})_{12}, \\ h_{jl} &= \frac{1}{(M_0^N)_{12}} \left[\frac{1}{2} (M_0^{N-j} M_2 M_0^{j-1})_{12} \delta_{jl} \right. \\ &\quad \left. + (1 - \delta_{jl}) (M_0^{N-l} M_1 M_0^{l-j-1} M_1 M_0^{j-1})_{12} \right]. \end{aligned} \quad (10)$$

The disorder-averaged reflectivity of the multilayer stack is obtained by combining Eq. (6) and (9) so that up to second order in the disorder we have

$$\begin{aligned} \langle R \rangle &= R_N \left[1 + 2\epsilon^2 \text{Re} \sum_{j=1}^N \left(c_j^2 + \frac{1}{2} |c_j|^2 - g_{jj} \right. \right. \\ &\quad \left. \left. - \frac{1}{2} (f_j + f_j^*) (c_j + c_j^*) + \frac{1}{2} |f_j|^2 + h_{jj} \right) \right], \end{aligned} \quad (11)$$

adopting the same reasoning employed for Eq. (8) above and with $R_N = |(M_0^N)_{12}/(M_0^N)_{22}|^2$ being the reflectivity of the N -layer stack in the absence of disorder ($\epsilon_j = 0$). Further note that the powers of M_0 entering T_N , R_N and the coefficients in Eqs. (7) and (10) encompassing the effects of the disorder can be computed directly through the relation

$$M_0^{\pm j} = U_{j-1}(\xi) M_0^{\pm 1} - U_{j-2}(\xi) \mathbb{K}, \quad (12)$$

with $U_j(\xi)$ being the Chebyshev polynomials of the second kind [5] and $\xi = \text{Tr}[M_0^{\pm 1}]/2$.

3. Geometric Disorder

We now apply the above results to a disordered photonic crystal where disorder affects the thickness of the spacer layer between the dielectric slabs viz. $(a-d) \rightarrow (a-d) + \epsilon_j$ with $|\epsilon_j| \ll (a-d)$, $\langle \epsilon_j \rangle = 0$ and the disorder strength being characterized by $\langle \epsilon_j^2 \rangle / (a-d)^2$. The refractive index n is otherwise constant ($n > 1$).

Just as discussed above, the transfer matrix of the j^{th} layer of this system is equal to

$$\begin{aligned} M_j &= \begin{pmatrix} e^{ik_0(a-d+\epsilon_j)} & 0 \\ 0 & e^{-ik_0(a-d+\epsilon_j)} \end{pmatrix} \mathcal{M} \\ &= (\cos(k_0 \epsilon_j) \mathbb{K} + i \sin(k_0 \epsilon_j) \sigma_z) M_0, \end{aligned} \quad (13)$$

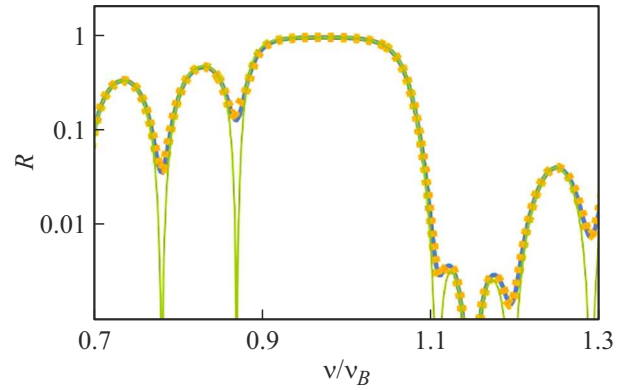


Figure 1. Reflectivity spectra near the first stop-band of a photonic crystal with geometric disorder: the green line is for the ideal case (no disorder), the thick blue line and the dotted orange line (almost superimposed) are for the disordered case calculated, respectively, with numerical averaging of the exact transfer matrix and with the perturbative approach of Eq. (11) (see text for details).

the matrix M_0 being the unit cell transfer matrix in the absence of disorder, as given by Eqs. (1), (2), and σ_z is the usual Pauli z matrix.

The total transfer matrix $M_T = \prod_{j=1}^N M_j$ can be expanded to second order in ϵ_j (disorder parameter) as

$$\begin{aligned} M_T &\simeq M_0^N \left(1 - \frac{1}{2} k_0^2 \sum_{j=1}^N \epsilon_j^2 \right) + ik_0 \sum_{j=1}^N \epsilon_j M_0^{N-j} \sigma_z M_0^j \\ &\quad - k_0^2 \sum_{j=1}^{N-1} \sum_{l=j+1}^N \epsilon_j \epsilon_l M_0^{N-l} \sigma_z M_0^{l-j} \sigma_z M_0^j, \end{aligned} \quad (14)$$

from which the coefficients in Eqs. (7) and (10) are identified as

$$\begin{aligned} c_j &= \frac{ik_0}{(M_0^N)_{22}} (M_0^{N-j} \sigma_z M_0^j)_{22}, \\ g_{jl} &= -(1 - \delta_{jl}) \frac{k_0^2}{(M_0^N)_{22}} (M_0^{N-l} \sigma_z M_0^{l-j} \sigma_z M_0^j)_{22} - \frac{1}{2} k_0^2 \delta_{jl}, \end{aligned} \quad (15)$$

and

$$\begin{aligned} f_j &= \frac{ik_0}{(M_0^N)_{12}} (M_0^{N-j} \sigma_z M_0^j)_{12}, \\ h_{jl} &= -(1 - \delta_{jl}) \frac{k_0^2}{(M_0^N)_{12}} (M_0^{N-l} \sigma_z M_0^{l-j} \sigma_z M_0^j)_{12} - \frac{1}{2} k_0^2 \delta_{jl}. \end{aligned} \quad (16)$$

Note that for uncorrelated disorder the coefficients $g_{j \neq l}$ and $h_{j \neq l}$ are immaterial, as discussed above, and only the matrices $M_0^{N-j} \sigma_z M_0^j$ are to be computed.

For illustrative purposes, we consider a photonic crystal with $d = 0.8a$, $n = 1.7$ and $N = 10$. In Fig. 1 we show the reflectivity spectrum around the first stop-band,

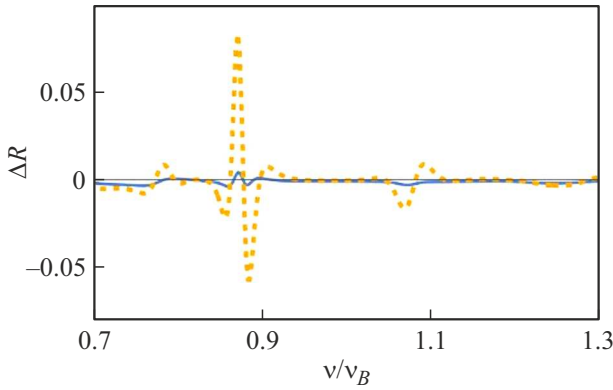


Figure 2. Difference between the reflectivity spectra of a photonic crystal with geometric disorder calculated with full numerical averaging and with Eq. (11): the dotted orange line is for a disorder level of 25 percent (the same as in Fig. 1), while the blue solid line is for a disorder level of 12 percent.

where $2\pi v_B/c = \pi/(a - d + nd)$, for the ideal case (thin green line) and a case with geometric disorder calculated either with a numerical configurational averaging of the exact transfer matrix (thick blue line) or with Eq. (11) (dotted orange line). Transmission spectra can likewise be obtained using Eq. (8) and simply add up to unity as the system is lossless. Geometric disorder is quantified setting $\epsilon_j = (a - d) \times 0.25 \times r_j$ where r_j is a random number uniformly distributed in the interval $[-1, +1]$, which implies a disorder level of 25 percent, and the reflectivity spectra are calculated either averaging over 1000 disorder realizations the exact transfer matrix or via the perturbative approach corresponding to Eq. (11). We hereafter deliberately use quite a large degree of disorder, significantly exceeding what is typically found in disordered photonic crystals, to assess the range of validity of the present perturbative approach. This point is further detailed in Sect. 5. As shown in Fig. 2 where the difference between the two calculations is plotted for two levels of disorder, the perturbative approach works very well.

4. Compositional disorder

The next special case is known as compositional disorder, here where the disorder affects only the refractive index value: $n \rightarrow n_0 + \epsilon_j$ with $n_0 > 1$, $|\epsilon_j| \ll (n_0 - 1)$ and again $\langle \epsilon_j \rangle = 0$, the disorder strength being characterised by $\langle \epsilon_j^2 \rangle / (n_0 - 1)^2$.

Then, as defined previously in Eqs. (3), (4), the single layer transfer matrix \mathcal{M} of Eq. (2) can be expanded to second order in the disorder ϵ_j , obtaining for the single cell

transfer matrix M_j

$$M_j \simeq \begin{pmatrix} e^{ik_0(a-d)} & 0 \\ 0 & e^{-ik_0(a-d)} \end{pmatrix} \left(\mathcal{M}_0 + \epsilon_j \mathcal{M}_1 + \frac{1}{2} \epsilon_j^2 \mathcal{M}_2 \right) \equiv M_0 + \epsilon_j M_1 + \frac{1}{2} \epsilon_j^2 M_2, \quad (17)$$

where \mathcal{M}_0 is simply given by Eq. (2) with n replaced by n_0 and the matrix derivatives, \mathcal{M}_1 and \mathcal{M}_2 can be conveniently written in terms of the usual σ Pauli matrices as

$$\begin{aligned} \mathcal{M}_1 &= -k_0 d \sin(k_0 d n_0) \mathbb{K} \\ &+ \frac{i}{2} \left(\frac{n_0^2 - 1}{n_0^2} \sin(k_0 d n_0) + \frac{n_0^2 + 1}{n_0} k_0 d \cos(k_0 d n_0) \right) \sigma_z \\ &- \frac{1}{2} \left(\frac{n_0^2 + 1}{n_0^2} \sin(k_0 d n_0) + \frac{n_0^2 - 1}{n_0} k_0 d \cos(k_0 d n_0) \right) \sigma_y, \end{aligned} \quad (18)$$

and

$$\begin{aligned} \mathcal{M}_2 &= -(k_0 d)^2 \cos(k_0 d n_0) \mathbb{K} \\ &+ \frac{i}{2} \left(2 \frac{n_0^2 - 1}{n_0^2} k_0 d \cos(k_0 d n_0) \right. \\ &+ \left. \left(\frac{2}{n_0^3} - \frac{n_0^2 + 1}{n_0} (k_0 d)^2 \right) \sin(k_0 d n_0) \right) \sigma_z \\ &- \frac{1}{2} \left(2 \frac{n_0^2 + 1}{n_0^2} k_0 d \cos(k_0 d n_0) \right. \\ &- \left. \left(\frac{2}{n_0^3} + \frac{n_0^2 - 1}{n_0} (k_0 d)^2 \right) \sin(k_0 d - n_0) \right) \sigma_y. \end{aligned} \quad (19)$$

Then, as in the previous two sections the total transfer matrix can be written to second order in the disorder parameter ϵ_j in the form of Eq. (5), with the coefficients due to disorder, c_j , g_{jl} , f_j , and h_{jl} identified as in Eqs. (7) and (10), and the reflectivity computed using Eq. (11). Again, for uncorrelated disorder as discussed above, only the matrices $(M_0^{N-j} M_1 M_0^{j-1})$ and $(M_0^{N-j} M_2 M_0^{j-1})$ are to be computed.

As a numerical example, we consider the same photonic crystal sample structure as above ($d = 0.8a$, $n_0 = 1.7$, $N = 10$) and show in Fig. 3 its reflectivity spectrum around the first stop-band (where $2\pi v_B/c = \pi/(a - d + n_0 d)$) for the ideal case (thin green line) and a case with compositional disorder calculated either with numerical configurational averaging of the exact transfer matrix (thick blue line) or with Eq. (11) (dotted orange line). Here, compositional disorder is introduced setting $\epsilon_j = (n_0 - 1) \times 0.13 \times r_j$ where r_j is a random number uniformly distributed in the interval $[-1, +1]$, which implies a compositional disorder level of 13 percent, and the reflectivity spectra are calculated either averaging over 1000 disorder realizations the exact transfer matrix or via the perturbative approach corresponding to Eq. 11. As evident from Fig.4 where the difference

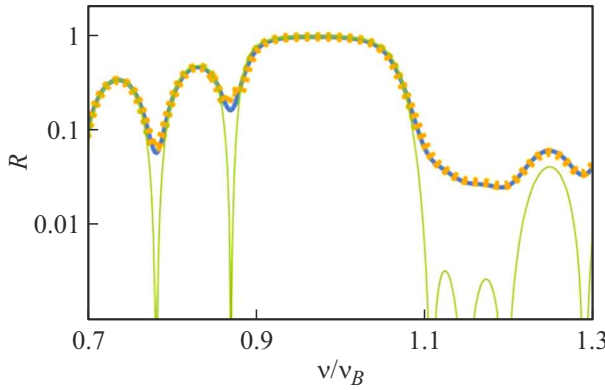


Figure 3. Reflectivity spectra near the first stop-band of a photonic crystal with compositional disorder: the green line is for the ideal case (the same as in Fig. 1), the thick blue line and the dotted orange line (almost superimposed) are for the disordered case calculated, respectively, with an exact transfer matrix and with the perturbative approach of Eq. (11) (see text for details).

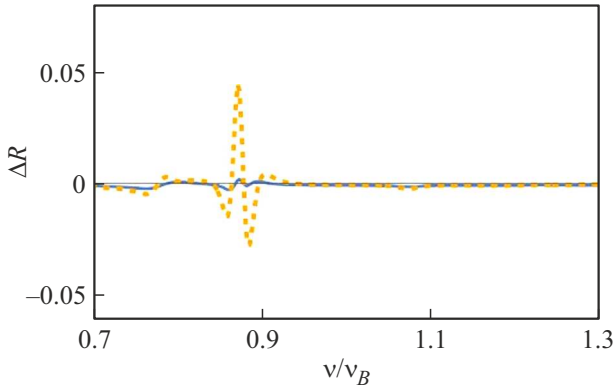


Figure 4. Difference between the reflectivity spectra of a photonic crystal with compositional disorder calculated with an exact transfer matrix and with Eq. (11): the dotted orange line is for a disorder level of 13 percent (the same as in Fig. 3, while the blue solid line is for a disorder level of 6 percent).

between the two calculations is shown for two levels of disorder, the perturbative approach works well also in this case, as discussed below.

5. Numerical accuracy

It might seem from a direct comparison of the blue solid line in Fig. 2 (12 percent geometric disorder) with the dotted orange line in Fig. 4 (13 percent compositional disorder) that the degree of accuracy of the perturbative approach would be worse for the latter case. However, the significance of the nominal disorder levels quoted above (e.g., 25 percent in Fig. 1 and 13 percent in Fig. 3) should be scrutinized as we do in the following. A better way to compare quantitatively the two disorder levels is to translate both of them into the respective typical phase variation they induce across the average period a for the specific

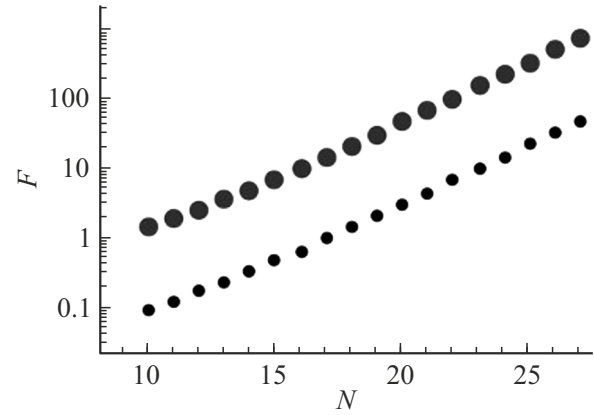


Figure 5. Grand averaging (F) of the norm Φ as a function of N (see text). Frequency averaging $F = \langle\langle f \rangle\rangle$ is over the gap spectral region while disorder averaging $f = \langle\Phi\rangle$ is for a 2% (small points) and 30% (large points) degree of geometric disorder. Other parameters are as in Figs. 1 and 2.

disordered systems considered above. For the case of geometric disorder, this phase variation is $\Delta\phi_g = k_0\sqrt{\langle\epsilon_j^2\rangle}$; for the case of compositional disorder, $\Delta\phi_c = k_0d\sqrt{\langle\epsilon_j^2\rangle}$. For the instances shown Fig. 1 and Fig. 3, it follows $\frac{\Delta\phi_g}{\Delta\phi_c} = \frac{25}{13}(\frac{a}{d}-1)\frac{1}{n_0-1} \simeq 0.7$, in turn the effective disorder level of the blue solid line in Fig. 2 is only about one third of that of the dotted orange line in Fig. 4. Thus, similar levels of effective disorder of both compositional and geometric type lead to a roughly comparable agreement between the exact and the perturbative approach.

Another important question is how long a sample the perturbative approach might handle. The generic expression Eq. (5) of the total transfer matrix of a photonic crystal of N cells can be written as

$$M_T \simeq M_0^N (\mathbb{K} + \Delta M(N)) \quad (20)$$

and is expected to hold provided ΔM , corresponding to the perturbative effects of disorder, remains small compared to \mathbb{K} , as assessed for instance by its Frobenius norm $\Phi = \sqrt{\sum_{i,j} |\Delta M_{i,j}|^2}$. For values of Φ comparable or larger than 1, the perturbative approach is not feasible. To assess its limits of validity, we consider averaging the norm Φ over disorder realizations, viz., $f = \langle\Phi\rangle$, in turn averaged over the photonic gap frequency range, viz., $F = \langle\langle f \rangle\rangle$ (grand averaging). Figure 5 reports F as a function of N averaged over 700 frequency values in the range $0.7\nu_B - 1.3\nu_B$ and for 1000 realizations of two degrees of geometric disorder.

It is clear that F increases roughly exponentially with N and that even for moderate values of N is much larger than 1. It is interesting to note, however, that even for the case $N = 10$ considered in Sect. 1, while for a disorder level of 2 percent F is actually small, for a disorder level of 30 percent it is comparable to 1, and yet even for a disorder level of 25 percent as shown in Fig. 1 the reflectivity

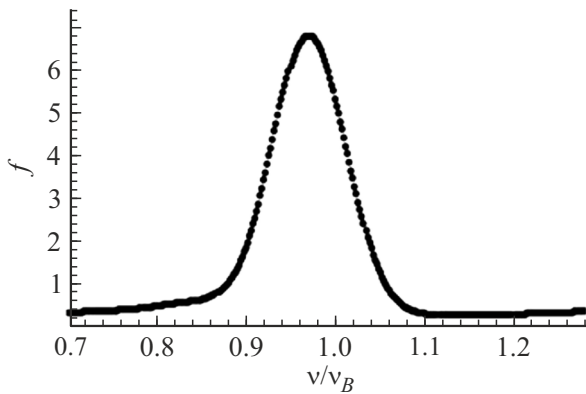


Figure 6. Disorder averaged f for a geometric disorder of 30 percent as a function of frequency for $N = 10$, other parameters are as in Figs. 1 and 2.

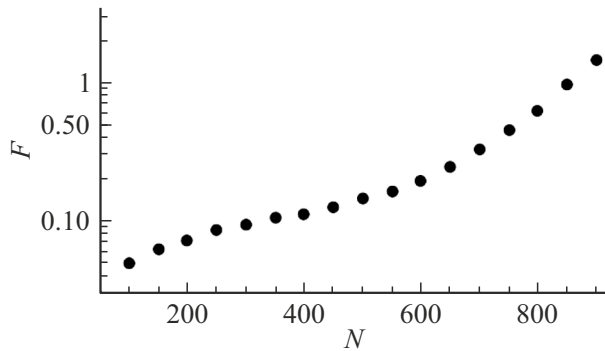


Figure 7. Grand averaging F for a compositional disorder levels of 30 percent and $n_0 = 1.01$ as a function of N , with $d = 0.8a$.

spectrum appears to be described reasonably well by the perturbative approach (see also Fig. 2). A similar behaviour is also observed for compositional disorder. This is due to the fact that the Frobenius norm Φ strongly depends on frequency and increases dramatically within the gap as shown in Fig. 6 where the average f of Φ over disorder realizations is shown as a function of frequency. In the high reflectivity frequency range around ν_B , R is close to one and is not much affected by disorder, while away from the gap the disorder perturbation matrix ΔM is actually small. As a matter of fact, the largest deviation of the reflectivity values calculated perturbatively from those obtained from an exact transfer matrix calculation occurs at the gap edges as shown in Fig. 2 and 4. Thus, in general, the reflectivity spectra turn out to be more accurate than expected on the basis of the frequency averaged F shown in Fig. 5.

For the parameter values considered so far, in particular the value of $n_0 = 1.7$ representative of a solid state based distributed Bragg reflector, the perturbative approach breaks down for moderate values of N of the order of a few tens. Another class of photonic crystals of current interest is that based on cold atoms loaded into optical lattices [3,4] for which only very small values of refractive index contrast are realistic, and samples containing a few hundred periods are

typically used. In the latter case, the perturbative approach works very well even for N values of the order of several hundreds as shown in Fig. 7.

6. Summary and conclusions

We have presented a semi-analytic, perturbative approach for calculating the effect of moderate disorder on the reflection and transmission from a multilayer. We note that already for a number of layers N on the order of one hundred, the perturbative approach for the reflectivity in Eq. (11) is computationally much more efficient than the usual one based on numerical configurational averaging. The computational shortcut here provided is essentially due to the fact that the coefficients c_j , g_{jl} , f_j , and h_{jl} appearing in Eq. (11) do not depend on disorder and are calculated only once, from which the disorder-averaged reflectivity is obtained analytically. The same applies for the transmittivity in Eq. (8). The present method is particularly suited to deal with atomic based photonic crystals [3–5], characterized by a low level of disorder and a high number of periods, especially when the single unit cell cannot be modeled as above by piece-wise constant optical response functions, but requires a more elaborate description [9,10].

References

- [1] J.D. Joannopoulos, S.J. Johnson, J.N. Winn, R.D. Mead. *Photonic Crystals: Molding the Flow of Light*. (Princeton University Press, 2008).
- [2] H.A. MacLeod. *Thin-Film Optical Filters*. (CRC Press, 2018).
- [3] I. Bloch. *Nat. Phys.*, **1**, 23 (2005).
- [4] J.-H. Wu, M. Artoni, G.C. La Rocca. *J. Opt. Soc. Am. B*, **25**, 1840 (2008).
- [5] S.A.R. Horsley, J.-H. Wu, M. Artoni, G.C. La Rocca. *Am. J. Phys.*, **82**, 206 (2014).
- [6] V.M. Agranovich, V.L. Ginzburg. Springer-Verlag (1984).
- [7] M. Artoni, G.C. La Rocca, F. Bassani. *Phys. Rev. E*, **72**, 046604 (2005).
- [8] R. Rengarajan, D. Mittleman, C. Rich, V. Colvin, *Phys. Rev. E*, **71**, 016615 (2005).
- [9] M. Artoni, G.C. La Rocca. *Phys. Rev. Lett.*, **96**, 073905 (2006).
- [10] J.-H. Wu, M. Artoni, G.C. La Rocca. *Phys. Rev. A*, **95**, 053862 (2017).
- [11] V.M. Agranovich, V.E. Kravtsov, I.V. Lerner. *Phys. Letts. A*, **125**, 435 (1987).
- [12] A.R. McGurn, K.T. Christensen, F.M. Mueller, A.A. Maradudin. *Phys. Rev. B*, **47**, 13120 (1993).
- [13] M.V. Berry, S. Klein. *Eur. J. Phys.*, **18**, 222 (1997).
- [14] M. Litinskaia, G.C. La Rocca, V.M. Agranovich, *Phys. Rev. B*, **64**, 165316 (2001).
- [15] M.A. Kaliteevski, D.M. Beggs, S. Brand, R.A. Abram, V.V. Nikolaev. *Phys. Rev. B*, **73**, 033106 (2006).
- [16] P. Michetti, G.C. La Rocca. *Phys. Rev. B*, **71**, 115320 (2005).
- [17] V.M. Agranovich, Yu.N. Gartstein. *Phys. Rev. B*, **75**, 075302 (2007).
- [18] A. Maurel, P.A. Martin. *Eur. Phys. J. B*, **86**, 486 (2013).